JACS
JOURNAL OF THE AMERICAN CHEMICAL SOCIETY

ARTICLE

pubs.acs.org/JACS

Odd−Even Effect of Repeating Aminoethylene Units in the Side Chain of N-Substituted Polyaspartamides on Gene Transfection Profiles

Hirokuni Uchida,[†] Kanjiro Miyata,[§] Makoto Oba,[∥] Takehiko Ishii,[†] Tomoya Suma,[†] Keiji Itaka,[§] Nobuhiro Nishiyama,[§] and Kazunori Kataoka*[,†,§,‡]

[†]Department of Bioengineering and [‡]Department of Materials Engineering, Graduate School of Engineering, The University of Tokyo, 7-3-1 Hongo, Bunkyo, Tokyo 113-8656, Japan

[§]Center for Disease Biology and Integrative Medicine, Graduate School of Medicine, The University of Tokyo, 7-3-1 Hongo, Bunkyo, Tokyo 113-0033, Japan

[∥]Department of Clinical Vascular Regeneration, Graduate School of Medicine, The University of Tokyo, 7-3-1 Hongo, Bunkyo, Tokyo 113-8655, Japan

Supporting Information

ABSTRACT: A series of the N-substituted polyaspartamides possessing repeating aminoethylene units in the side chain was prepared in this study to identify polyplexes with effective endosomal escape and low cytotoxicity. All cationic N-substituted polyaspartamides showed appreciably lower cytotoxicity than that of commercial transfection reagents. Interestingly, a distinctive odd−even effect of the repeating aminoethylene units in the polymer side chain on the efficiencies of endosomal escape and transfection to several cell lines was observed. The polyplexes from the polymers with an even number of repeating aminoethylene units (PA-Es) achieved an order of magnitude higher transfection efficiency, without marked cytotoxicity, than those of the polymers with an odd number of repeating aminoethylene units (PA-Os). This odd−even effect agreed well with the buffering capacity of these polymers as well as their capability to disrupt membrane integrity selectively at endosomal pH, leading to highly effective endosomal escape of the PA-E polyplexes. Furthermore, the formation of a polyvalent charged array with precise spacing between protonated amino groups in the polymer side chain was shown to be essential for effective disruption of the endosomal membrane, thus facilitating transport of the polyplex into the cytoplasm. These data provide useful knowledge for designing polycations to construct safe and efficient nonviral gene carriers.

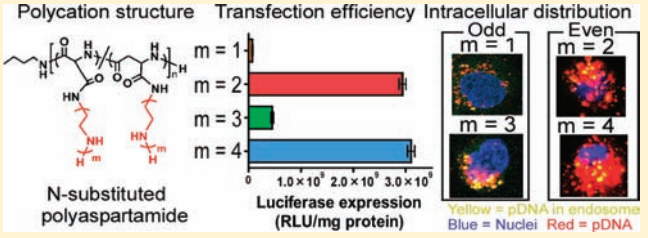

INTRODUCTION

Gene therapy has received considerable attention because of its significant potential to treat intractable diseases; however, the development of safe and efficient carriers of plasmid DNA (pDNA) remains a critical issue.[1,2] Among pDNA carriers, polyion complexes (PICs) formed between negatively charged DNA and polycations, which are termed "polyplexes", have been extensively studied.[3−8] Such polyplexes are required to stably deliver pDNA to the nuclei in the target cells. However, the most critical issue affecting the trafficking of polyplexes is the inefficient translocation from the endosomes to the cytoplasm after internalization through the endocytosis.[9] Hence, considerable efforts have been devoted to the development of polycations with potent endosomal escape ability.[10−15] However, such polycations often cause severe cytotoxicity.[16] Therefore, the fine-tuning the chemical structures of polycations to enhance their endosomal escape ability while cytotoxicity is reduced is a major key in designing polyplexes; this proves to be a challenge with respect to various fields of chemistry.

Linear polyethylenimine (linear PEI) is one of the most widely used polycations possessing potent endosomal escape ability.[17−20] Indeed, linear PEI polyplexes have been examined in several disease models to evaluate their clinical applications.[21] Linear PEI consists of repeating aminoethylene units and features a relatively low pK_a.[22] Hence, the protonation degree of linear PEI increases when pH decreases from the extracellular pH (∼7.4) to the endosomal pH (∼5.5). This facilitates the endosomal escape of linear PEI polyplexes because of endosomal disruption caused by increased osmotic pressure in the endosome (the so-called proton sponge effect[12,17]) and/or perturbation of the endosomal membrane caused by a direct interaction with polycations.[23−26] Thus, linear PEI exhibits a relatively high transfection efficiency but consequently induces considerable cytotoxicity because of interactions with biomolecules including the plasma membrane.[16,27] In order to solve this cytotoxicity problem, we have truncated a defined number of repeating aminoethylene units and introduced them into the side chain of the N-substituted polyaspartamides to obtain fine-tuned polycations achieving efficient gene transfection but reduced cytotoxicity. In our previous study,

Received: May 16, 2011
Published: August 31, 2011

Scheme 1. Synthesis of PAsp(EDA), PAsp(DET), PAsp(TET), and PAsp(TEP) by Aminolysis of PBLA

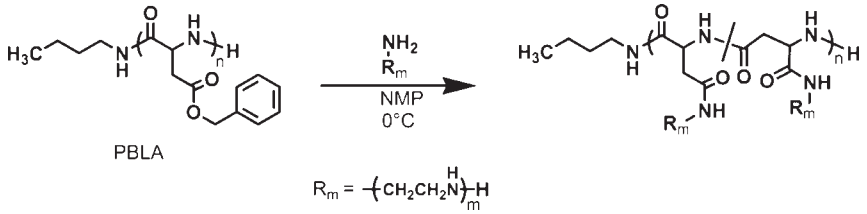

poly{*N*-[*N*′-(2-aminoethyl)-2-aminoethyl]aspartamide} possessing two repeating aminoethylene units [−(CH_2−CH_2−NH)$_2$−H] was synthesized by the introduction of diethylenetriamine (DET) (bis(2-aminoethyl)amine) [PAsp(DET)] into the side chain of the N-substituted polyaspartamide.[28] PAsp(DET) showed minimal membrane destabilizing ability with a monoprotonated side chain at pH 7.4 but a potent membrane destabilizing effect with a diprotonated side chain at pH 5.5. Thus, PAsp(DET) is assumed to selectively damage the endosomal membrane, thus enabling less toxic gene transfer in various cells including fragile primary culture cells.[26] Furthermore, the in vivo efficacy of gene transfer using PAsp(DET) has been demonstrated in several disease models.[29,30]

These studies motivated us to further investigate the relationship between the protonation behavior and biological properties of the N-substituted polyaspartamides possessing repeating aminoethylene units in the side chain. We expect such studies to provide useful knowledge for designing polycations that are safe and efficient nonviral gene carriers. Therefore, in this study, we examined various N-substituted polyaspartamides possessing different numbers of repeating aminoethylene units in the side chain and evaluated the relationship between their protonated states at pH 7.4 and 5.5 and their biological properties such as the hemolytic activity, cytotoxicity, endosomal escape ability, and transfection efficiency. Interestingly, a distinctive odd−even effect associated with the number of aminoethylene units was observed on the efficiencies of endosomal escape and in vitro transfection. The polyplexes from the N-substituted polyaspartamides possessing even-numbered repeating aminoethylene units (PA-Es) achieved transfection efficiencies, without marked cytotoxicity, that were an order of magnitude higher than those from the N-substituted polyaspartamides possessing odd-numbered repeating aminoethylene units (PA-Os). The mechanism for endosomal escape of these N-substituted polyaspartamide polyplexes was examined in detail to explain this interesting odd−even effect.

RESULTS

Synthesis and Characterization of N-Substituted Polyaspartamides. Introduction of repeating aminoethylene units into the poly(β-benzyl-L-aspartate) (PBLA) side chain was performed by the aminolysis reaction of PBLA with ethylenediamine (EDA), diethylenetriamine (DET), triethylenetetramine (TET), or tetraethylenepentamine (TEP), as previously reported,[31] and we synthesized poly[*N*-(2-aminoethyl)aspartamide] [PAsp(EDA)], PAsp(DET), poly(*N*-{*N*′-[*N*″-(2-aminoethyl)-2-aminoethyl]-2-aminoethyl}aspartamide) [PAsp(TET)], and poly-[*N*-(*N*′-{*N*″-[*N*‴-(2-aminoethyl)-2-aminoethyl]-2-aminoethyl}-2-aminoethyl)aspartamide] [PAsp(TEP)] (Scheme 1). It is noteworthy that in this way a series of N-substituted cationic polyaspartamides, with the same polymerization degree and molecular weight distribution, was readily obtained.[32] Each N-substituted cationic polyaspartamide is abbreviated as PAsp-(R), in which R denotes the abbreviation of the amines substituted in the side chain. The quantitative aminolysis of the side chain was confirmed from the peak intensity ratio of the protons from the methyl group at the α-chain end of the polymer ($CH_3CH_2CH_2CH_2$−, δ = 0.9 ppm) to all the methylene protons in the side chains (δ = 2.7−3.6 ppm) in the ^{1}H NMR spectra (Figure 1).

pH-Dependent Change in the Degree of Protonation (α) of Amino Groups in the Side Chain of N-Substituted Polyaspartamides. In order to estimate the protonation states of the amino groups in the side chain of the N-substituted polyaspartamide (hereafter, the polymer), potentiometric titration was performed in the pH range 1.2−11.5 in a 150 mM NaCl solution at 37 °C. The resultant titration curves were converted to differential curves to determine each neutralization point (data not shown). The total molar amount of consumed NaOH in the titration of PAsp(EDA) and PAsp(DET) corresponded well to the residual molar amount of amino groups of each polymer (5 mmol) in the solution, indicating that all the amino groups of the polymer were protonated at the beginning (pH 1.2) and deprotonated at the end (pH 11.5). Accordingly, the degree of protonation (α) and p*K* (=pH + log[α/(1 − α)]) were calculated and plotted against pH and α, respectively (Figure 2). On the other hand, the molar amount of consumed NaOH for the titration of PAsp(TET) and PAsp(TEP) was substantially lower than the residual molar amount of amino groups in the solution, suggesting that the amino groups in PAsp(TET) and PAsp-(TEP) should not be fully protonated, even at pH 1.2. Thus, the α/pH and p*K*/α curves of these polymers were calculated from the neutralization point in the differential curve and also shown in Figure 2. The change in the degree of protonation between pH 7.4 and 5.5 (Δα), indicating the buffering capacity, was calculated for each polymer from the values of α at pH 7.4 and 5.5 and is summarized in Table 1. Obviously, PAsp(DET) showed the largest Δα, followed by PAsp(TEP), PAsp(TET), and PAsp-(EDA). The number of protonated amines in each polymer (NA) at the corresponding pH was also calculated from α and the number of residual amino groups in the polymer by the following equation: NA = α*n* × 102, where *n* is the repeating number of aminoethylene units in the polymer side chain and 102 is the averaged polymerization degree. Furthermore, the averaged cationic charge density (CD) of each polymer was defined as the ratio of the NA to the number-averaged molecular weight (M_n) of the polymers (Table 1). The pK_a values for each protonation step were determined from the p*K*/α curves and are summarized in Table 1. Note that the p$K_{a4,TEP}$ value was not determined because the fourth protonation of the residual amino

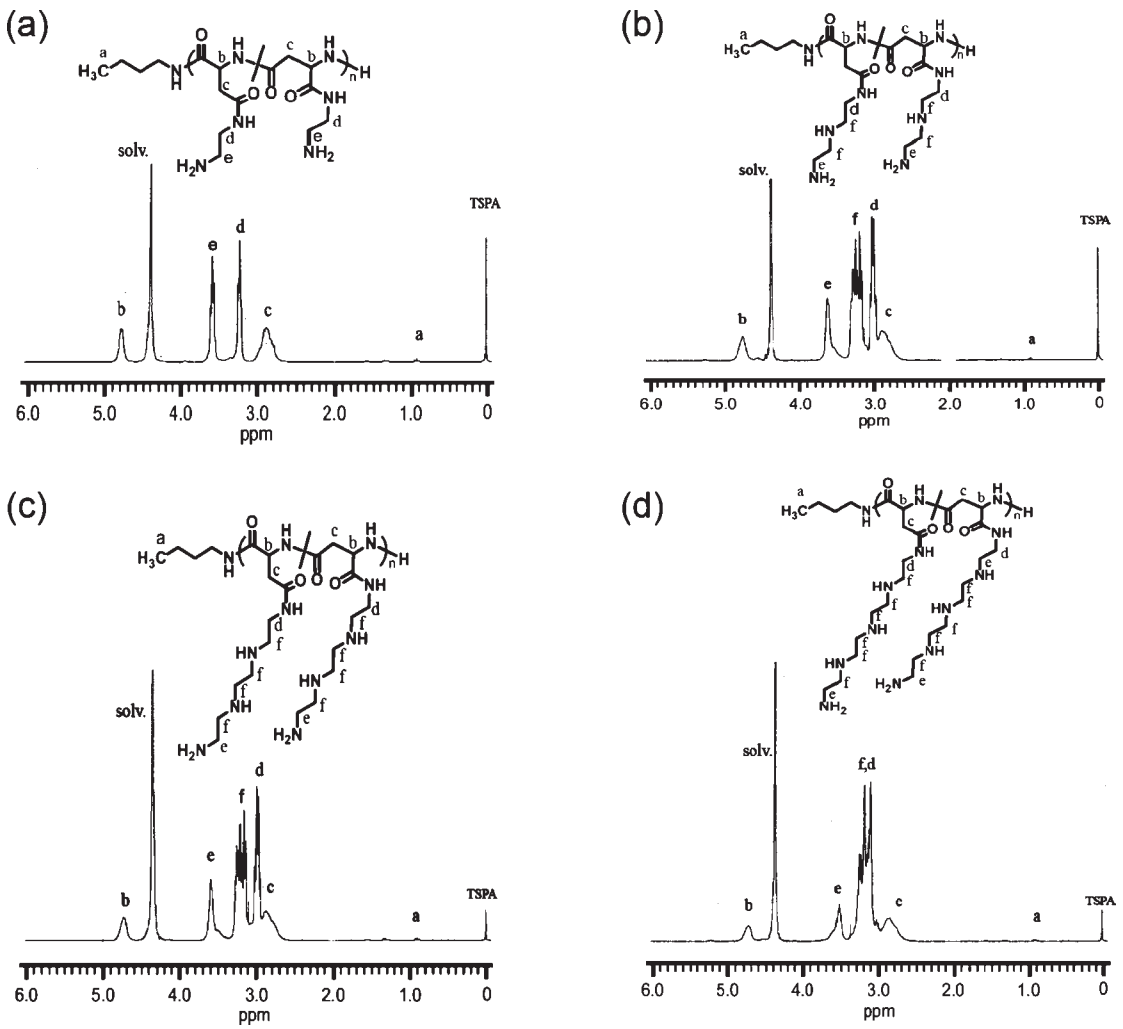

Figure 1. ^{1}H NMR spectra of (a) PAsp(EDA), (b) PAsp(DET), (c) PAsp(TET), and (d) PAsp(TEP). Solvent, D_2O; temperature, 70 °C; polymer concentration, 10 mg/mL.

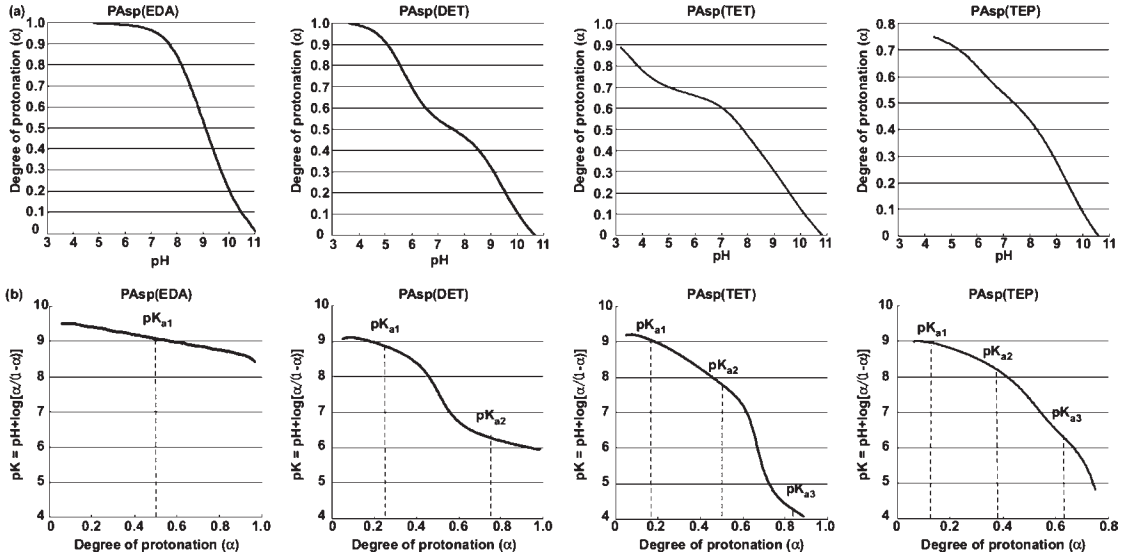

Figure 2. (a) α/pH curves and (b) pK_a/α curves of each N-substituted polyaspartamide in 150 mM NaCl solution at 37 °C.

dx.doi.org/10.1021/ja204466y |*J. Am. Chem. Soc.* 2011, 133, 15524–15532

Table 1. Physicochemical Parameters of the N-Substituted Polyaspartamides at pH 7.4 and 5.5

	α			number of protonated amines (NA[a])		charge density (CD[b])				
polymer	pH 7.4	pH 5.5	$\Delta\alpha$	pH 7.4	pH 5.5	pH 7.4	pH 5.5	pK_{a_1}	pK_{a_2}	pK_{a_3}
PAsp(EDA)	0.93	0.99	0.06	94	100	0.00538	0.00621	9.0		
PAsp(DET)	0.51	0.82	0.31	104	167	0.00505	0.00811	8.9	6.2	
PAsp(TET)	0.56	0.66	0.10	171	205	0.00682	0.00817	9.1	7.8	4.3
PAsp(TEP)	0.49	0.68	0.17	199	277	0.00673	0.00936	9.0	8.2	6.3

[a] NA = α × (the repeating number of aminoethylene units in the polymer side chain) × (the polymerization degree). [b] The ratio of the NA to the number-averaged molecular weight (M_n) of polymers.

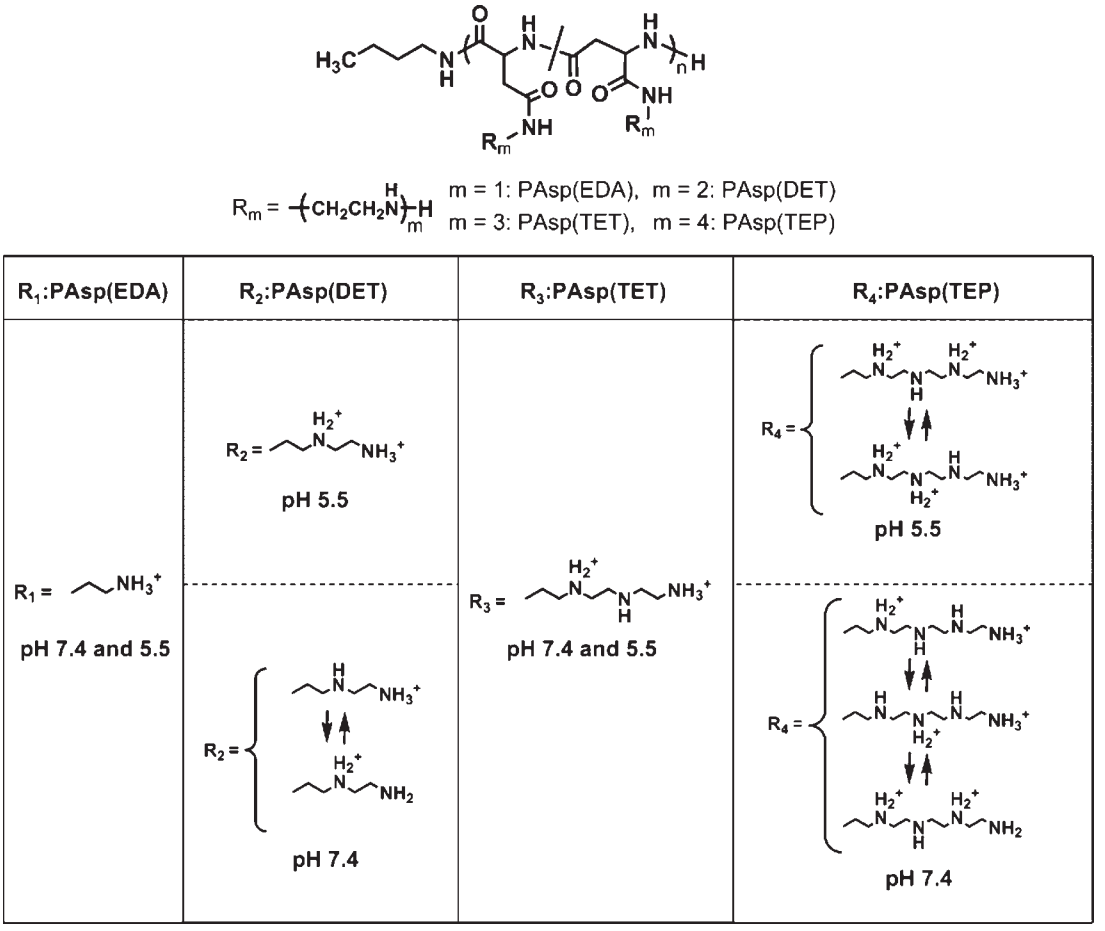

Figure 3. Major protonated structures of amino groups in the side chain of each polyaspartamide at pH 7.4 and 5.5.

groups in PAsp(TEP) was substantially limited, even at pH 1.2. Eventually, the major protonated structures of these polymers under physiological (pH = 7.4) and endosomal (pH = 5.5) conditions were estimated as shown in Figure 3.

Membrane Destabilizing Activity of N-Substituted Polyaspartamides. Our previous study revealed that PAsp(DET) disturbs the integrity of cellular membranes selectively at endosomal acidic pH presumably because of the transition of the side chain diamine unit from a monoprotonated to diprotonated state, which enhances the local charge density and facilitates the interaction with cellular membranes.[26] To determine the membrane-destabilizing activities of the N-substituted polyaspartamides as well as linear PEI (ExGen 500), the hemolysis assay was performed by mixing these polymers with murine erythrocytes at pH 7.4 and 5.5, at which extracellular neutral and endosomal acidic conditions, respectively, were simulated. As shown in Figure 4, ExGen 500 showed a considerably high hemolysis ratio (approximately 30%) at pH 7.4, which may be correlated with its high cytotoxicity. In contrast, all polymers induced substantially low hemolysis (less than 5%) at pH 7.4. Alternatively, at pH 5.5, the polymers possessing even-numbered repeating aminoethylene units [PAsp(DET) and PAsp(TEP)] and ExGen 500 significantly enhanced the hemolytic activity, whereas those possessing odd-numbered repeating units [PAsp(EDA) and PAsp(TET)] showed no significant increase. Thus, a unique odd−even effect of the repeating number of aminoethylene units was clearly observed for the pH-dependent hemolytic activity of a series of N-substituted polyaspartamides. Furthermore, the hemolytic

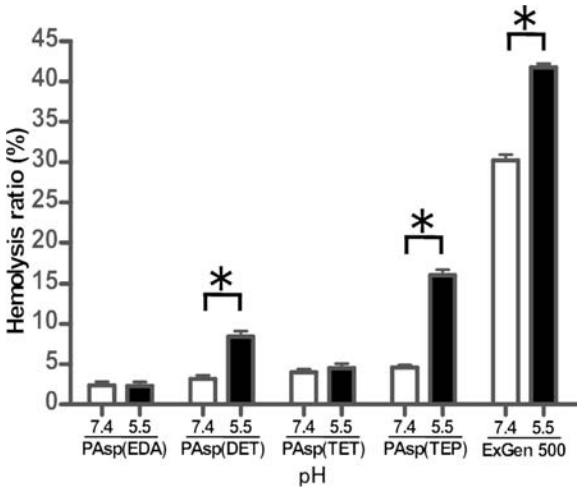

Figure 4. Hemolytic activity of PAsp(EDA), PAsp(DET), PAsp(TET), PAsp(TEP), and ExGen 500 ([amine] = 5 mM) against murine erythrocytes at pH 7.4 and 5.5. Results are expressed as mean ± SEM (N = 4). *P < 0.05.

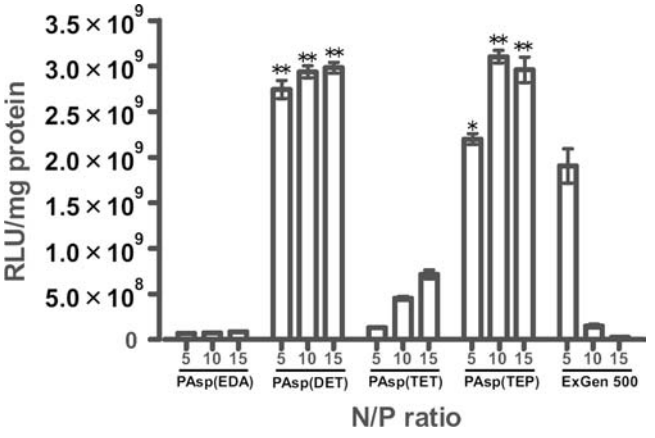

Figure 5. In vitro transfection efficiency of PAsp(EDA), PAsp(DET), PAsp(TET), PAsp(TEP), and ExGen 500 polyplexes at varying N/P ratios with Huh-7 cells determined by luciferase assay. Results are expressed as mean ± SEM (N = 4). * indicates that polyplexes show a significantly higher transfection efficiency than the PA-Os polyplexes at the same N/P ratio (P < 0.01), ** indicates that polyplexes show a significantly higher transfection efficiency than the PA-Os polyplexes at the same N/P ratio (P < 0.01) and the ExGen 500 polyplexes at N/P = 5 (P < 0.05).

activities of the polyplexes from the N-substituted polyaspartamides and ExGen 500 were determined at N/P = 10, which corresponds to the residual molar ratio of the amino groups in polycations to the phosphate groups in pDNA (Figure 1, Supporting Information). The hemolytic activity of polyplexes showed a similar odd−even effect, indicating that the membrane-destabilizing activity of the polycations was maintained even after the formation of polyplexes.

Size and ζ-Potential of Polyplexes Prepared from pDNA and N-Substituted Polyaspartamides. The polyplexes from the N-substituted polyaspartamides were characterized by measuring the ζ-potential and hydrodynamic diameter at pH 7.4 and 37 °C (Figure 2, Supporting Information). At N/P ratios above 4, all polyplexes had a similar size of approximately 100 nm with a

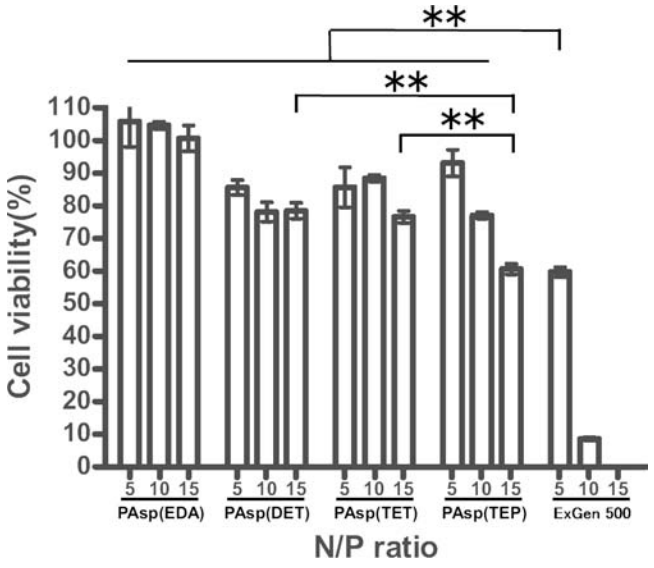

Figure 6. Cell viability assay of Huh-7 cells incubated with PAsp(EDA), PAsp(DET), PAsp(TET), PAsp(TEP), and ExGen 500 polyplexes under the same experimental conditions as in Figure 5. Results are expressed as mean ± SEM (N = 4). **P < 0.01.

constant ζ-potential of approximately 30 mV. Note that the formation of large aggregates around 1 μm was observed in each polyplex at a specific N/P ratio. Because each polyplex exhibited a ζ-potential close to neutral at this N/P ratio, large aggregate formation is expected to be due to decreased colloidal stability induced by charge neutralization. In the following experiments, the polyplexes prepared at N/P ratios above 4 were used because they apparently have similar physicochemical characteristics.

In Vitro Transfection and Cytotoxicity. The transfection efficiency of the luciferase gene in human hepatoma cells (Huh-7) was compared among the polyplexes prepared from PAsp(EDA), PAsp(DET), PAsp(TET), and PAsp(TEP) at N/P = 5, 10, and 15 (Figure 5). The polyplex from a linear PEI-based commercial transfection reagent (ExGen 500) was used as a control. Remarkable transfection efficiencies, which were higher than the maximum value obtained by ExGen 500 at N/P = 5, were achieved by polyplexes from PAsp(DET) (over N/P = 5) and PAsp(TEP) (over N/P = 10) possessing the even-numbered repeating aminoethylene units (PA-Es) (P < 0.05). Furthermore, polyplexes from PA-Es [PAsp(DET) and PAsp(TEP)] revealed significantly higher transfection efficiencies than those from PA-Os [PAsp(EDA) and PAsp(TET)] at all of the examined N/P ratios (P < 0.01). This remarkable odd−even effect on transfection efficiencies was not only limited to Huh-7 cells but was also observed for a human lung adenocarcinoma epithelial cells (A549) and a human umbilical vein endothelial cells (HUVEC) (Figure 3, Supporting Information). Note that a drastic reduction in the transfection efficiency was observed for the ExGen 500 polyplexes at higher N/P ratios, whereas it was not observed for any polyplexes from the N-substituted polyaspartamides. The substantially decreased transfection efficiency in the ExGen 500 polyplexes at higher N/P ratios is believed to be a direct result of severe cytotoxicity, as shown in Figure 6. In contrast, all polyplexes from the N-substituted polyaspartamides maintained a cell viability over 85% at N/P = 5 and over 75% even at N/P = 15, except for the polyplex from PAsp(TEP) at N/P = 15 (60%). Indeed, significant differences between the polyplexes from ExGen 500 at

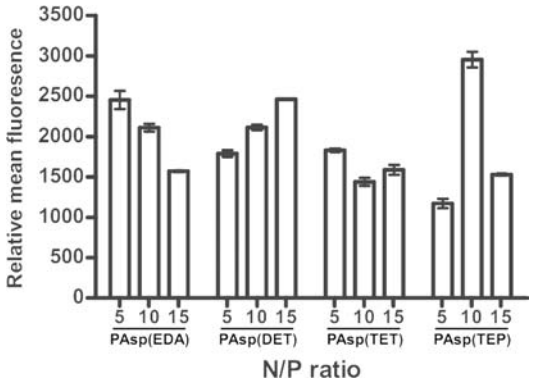

Figure 7. Cellular uptake of Cy5-labeled pDNA complexed with N-substituted polyaspartamides at various N/P ratios after 24 h incubation with Huh-7 cells (10 000 cells). Results are expressed as mean ± SEM ($N = 4$).

N/P = 5 and other N-substituted polyaspartamides except PAsp(TEP) at N/P = 15 were observed ($P < 0.01$). Polyplexes from PAsp(TEP) showed significantly lower cell viability than those from PAsp(DET) and PAsp(TET) at N/P = 15 ($P < 0.01$), indicating higher cytotoxicity with an increase in the N/P ratio.

Cellular Uptake of Polyplexes Determined by Flow Cytometry. The transfection efficiency of the polyplexes is often correlated with their cellular uptake. Thus, we compared the cellular uptake of each polyplex containing Cy5-labeled pDNA using flow cytometry. The histogram of flow cytometry revealed that almost 100% of the cells underwent polyplex uptake (data not shown). Figure 7 shows the relative mean fluorescence for the cellular uptake of Cy5-labeled pDNA, which apparently does not correlate with the transfection efficiency (Figure 5). Indeed, despite the significantly lower transfection efficiency, the polyplexes from PAsp(EDA) and PAsp(TET) showed levels of cellular uptake similar to those from PAsp(DET) and PAsp(TEP).

Intracellular Trafficking of Polyplexes Observed by Confocal Laser Scanning Microscopy (CLSM). Intracellular trafficking of each polyplex (N/P = 10) containing Cy5-labeled pDNA (red) was monitored particularly for endosomal localization by CLSM after staining the late endosome and lysosome with LysoTracker Green (green) and the nucleus with Hoechst 33342 (blue) (Figure 8a,b). In the overlay images, the yellow pixels represent the colocalization of Cy5-labeled pDNA with the late endosome/lysosome. Note that in our previous CLSM study Cy5-labeled pDNA in the poly(L-lysine) polyplex, which was used as the negative control and lacks endosomal escape ability, was found to maintain colocalization with the late endosome/lysosome throughout the observation period. This result provided the basis for estimating the endosomal escape ability of examined polyplexes from the decrease in the colocalization ratio estimated from the CLSM data.[26] Eventually, PAsp(DET) and PAsp(TEP) polyplexes appeared to disperse more efficiently in the entire cytoplasmic region than other polyplexes from the polymers with the odd-numbered repeating aminoethylene units in the side chains. As shown in Figure 8c, PAsp(EDA) and PAsp(TET) polyplexes showed an increase in the colocalization ratio until 12 and 24 h, respectively, indicating that the major fraction of PA-O polyplexes might be trapped in the lysosome. In contrast, PAsp(DET) and PAsp(TEP) polyplexes showed colocalization ratios lower than those of PAsp(EDA) and PAsp(TET) polyplexes at all time points. Also, PAsp(DET) and PAsp(TEP) polyplexes showed a decrease in the colocalization ratio after 12 and 6 h incubation, respectively, suggesting that the major fraction of PA-E polyplexes might escape from the endosome. At 12 h, the colocalization ratio of PAsp(DET) polyplexes was significantly lower than those of PAsp(EDA) and PAsp(TET) polyplexes ($P < 0.05$). At 24 and 48 h, the colocalization ratio of PAsp(TEP) polyplexes was significantly lower than that of PAsp(DET) polyplexes ($P < 0.05$ at 24 h, $P < 0.01$ at 48 h), indicating that the most efficient endosomal escape was for PAsp(TEP) polyplexes. Furthermore, the Manders coefficients were calculated using Image J software (http://rsbweb.nih.gov/ij/) to evaluate the colocalization of Cy5-labeled pDNA and LysoTracker after 48 h incubation. Note that the coefficients range between 0 and 1, which indicates no overlap and full overlap, respectively, and a higher value indicates that a larger fraction of polyplexes is trapped in the endosome/lysosome. The coefficients were calculated to be 0.549 for PAsp(EDA), 0.381 for PAsp(DET), 0.498 for PAsp(TET), and 0.345 for PAsp(TEP), consistent with the endosome colocalization ratios in Figure 8c. From these results, we conclude that the polyplexes from the polymer possessing the even-numbered repeating aminoethylene units enable the efficient endosomal escape of complexed pDNA into the cytoplasm, which agrees well with the transfection results shown in Figure 5.

DISCUSSION

In this study, to elucidate the precise structure−function relationship of the polyplexes, we synthesized a series of N-substituted polyaspartamides with increasing numbers of repeating aminoethylene units in the side chain: PAsp(EDA), PAsp(DET), PAsp(TET), and PAsp(TEP) (one to four repeating aminoethylene unit(s), respectively). The polyplexes from these N-substituted polyaspartamides were confirmed to have a similar size (~100 nm) and ζ-potential (~30 mV) at N/P ratios >4 (Figure 2, Supporting Information), suggesting similar fundamental physicochemical properties. The in vitro transfection experiment with Huh-7 cells exhibited a distinctive odd−even effect with respect to the number of repeating aminoethylene units: the polyplexes from the polymer with the even-numbered repeating aminoethylene units (PA-E) showed appreciably higher transfection efficiencies without marked cytotoxicity compared to polymers with odd-numbered repeating aminoethylene units (PA-O) (Figures 5 and 6).

To elucidate the reasons for this unique odd−even effect, we examined the cytotoxicity, cellular uptake, and endosomal escape behaviors of each polyplex. While the cell viability (Figure 6) and cellular uptake (Figure 7) profiles were similar between the polyplexes from both PA-E and PA-O, a significant difference in the endosomal escape behavior as determined from CLSM imagery was observed between the two variants. PA-E [PAsp(DET) and PAsp(TEP)] polyplexes revealed lower endosomal colocalization and higher dispersion into the cytoplasm than PA-O [PAsp(EDA) and PAsp(TET)] polyplexes (Figure 8), indicating that the higher transfection efficiency of the PA-E polyplexes is strongly correlated with their capability of endosomal escape.

Several previous studies revealed that the endosomal escape of the polyplexes may be facilitated by an increased osmotic pressure in the endosome because of a buffering effect associated with the amino groups in the constituent polycations (proton sponge hypothesis).[12,17] Accordingly, we examined the relationship between the buffering capacity of amino groups in the

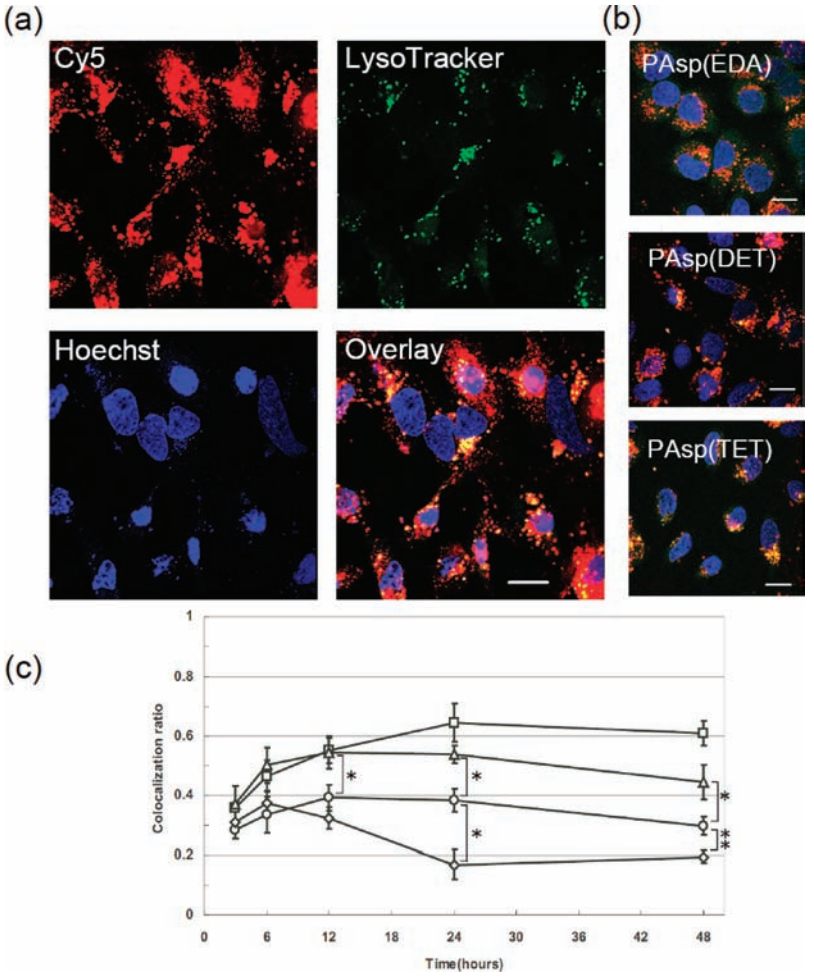

Figure 8. (a) Intracellular distribution of Cy5-labeled pDNA (red) complexed with PAsp(TEP) at N/P = 10 for Huh-7 cells after 48 h incubation. Acidic late endosomes and lysosomes were stained with LysoTracker Green (green). The nuclei were stained with Hoechst 33342 (blue). The scale bar represents 20 μm. (b) Overlay images of Cy5-labeled pDNA, LysoTracker Green, and Hoechst 33342 in Huh-7 transfected with the polyplexes from PAsp(EDA), PAsp(DET), and PAsp(TET) observed under the same conditions as those of part a. (c) Time-dependent changes in colocalization ratios of the PAsp(EDA) (square), PAsp(DET) (circle), PAsp(TET) (triangle), and PAsp(TEP) (diamond) polyplexes containing Cy5-labeled pDNA with late endosomes and lysosomes. Results are expressed as mean ± SEM (N = 10). *P < 0.05, **P < 0.01.

N-substituted polyaspartamides and the endosomal escape efficiency of their polyplexes. The buffering capacity was estimated from the change in the degree of protonation between pH 7.4 and 5.5 ($\Delta\alpha$) (Table 1) and was consistent with the observed odd−even effect. PA-Es [$\Delta\alpha$ = 0.31 and 0.19 for PAsp(DET) and PAsp(TEP), respectively] possess higher buffering capacities than PA-Os [$\Delta\alpha$ = 0.06 and 0.11 for PAsp(EDA) and PAsp(TET), respectively]. The assumed protonated structures of the side chains for each polymer (Figure 3) are rather interesting. Almost all the amino groups in the PAsp(EDA) side chains are protonated, regardless of pH (7.4 or 5.5). On the other hand, most of the PAsp(DET) side chains are in the monoprotonated state at pH 7.4 (α = 0.51) and diprotonated state at pH 5.5 (α = 0.82) owing to the appreciable difference in pK_{a_1} (8.9) and pK_{a_2} (6.2), as reported in our previous paper.[26] Low pK_{a_2} values in PAsp(DET) are due to the thermodynamic disadvantages of the diprotonated structure in 1,2-diaminoethane caused by electrostatic repulsion between the two protonated amines, locking the conformation in the *anti* form with less rotational freedom (butane effect). The absence of a significant change in α for PAsp(TET) with pH ($\Delta\alpha$ = 0.11) may be explained in a similar way: the fully protonated (triprotonated) structure of an *N*-(2-aminoethyl)-1,2-diaminoethane unit has a substantial thermodynamic penalty because of the strong repulsive force from the two neighboring protonated amines. Consequently, the side chain prefers to exist as a diprotonated structure with diethyleneamine spacing ($-NH_2^+-CH_2-CH_2-NH-CH_2-CH_2-NH_3^+$) containing a nonprotonated amino group in the center even at lower pH. Alternatively, for PAsp(TEP), α increases from 0.49 to 0.68 with a decrease in pH from 7.4 to 5.5 because the pK_{a_3} value (6.3) exists between these two pH values. As shown in Figure 3, the dominant structure changes from a diprotonated state at pH 7.4 to a triprotonated state at pH 5.5. The latter form, with its integrated positive charge, is still allowed under acidic conditions possibly because the increase in electrostatic repulsion accompanying the third protonation may be alleviated by sufficient length and rotational flexibility of the diethyeleneamine spacing ($-CH_2CH_2NHCH_2CH_2-$). Note that pK_{a_4} of PAsp(TEP) is much lower than the titration range (pH < 1.2) because of the highly repulsive nature of the fully protonated structure.

Although the buffering capacity may explain the odd−even effect observed in the transfection efficiency of the examined

polyplexes, it does not completely agree with the order of their endosomal escape efficiency. PAsp(DET) possessed relatively larger $\Delta\alpha$ than PAsp(TEP); however, the polyplex from the latter achieved significantly higher endosomal escape efficiency (lower endosomal colocalization ratio) than that from the former (Figure 8), suggesting the presence of an additional factor affecting the endosomal escape behavior of the polyplexes. In this regard, membrane destabilization directly by polycation interaction should be emphasized, as indicated from the result of the hemolysis assay shown in Figure 4. The odd−even effect was clearly observed in this assay and only the PA-E series induced a substantial increase in hemolysis at acidic pH. PAsp(TEP) demonstrated the highest hemolysis (14.4%), followed by PAsp(DET) (8.0%), PAsp(TET) (4.9%), and PAsp(EDA) (1.8%). The order of hemolytic activity at pH 5.5 agrees well with the endosomal escape efficiency of the polyplexes (Figure 8), suggesting that disturbing the membrane integrity may be important for the endosomal escape of these polyplexes. Furthermore, the weak hemolytic activity for each polymer at pH 7.4 agrees with their low cytotoxicity (Figure 6), suggesting their limited interaction with plasma membranes of mammalian cells under physiological conditions. Note that ExGen 500 also showed the membrane destabilizing activity in response to the acidic pH in the endosome (Figure 4). Nevertheless, it is assumed that the considerably high hemolytic activity (approximately 30%) of ExGen 500 at pH 7.4 may be correlated with its high cytotoxicity (Figure 6), suggesting that the augmentation of repeating aminoethylene units might increase cytotoxicity regardless of pH.

To further discuss the mechanism for cellular membrane destabilization induced by the N-substituted polyaspartamides, we focus here on the number of protonated amines (NA) and the overall cationic charge density (CD) in each polymer strand (Table 1). A previous study revealed that polycations with larger NA and higher CD tend to induce stronger disturbances in the membrane integrity, presumably resulting from a higher affinity of the plasma membrane for positively charged components.[33] Yet the calculated NA and CD were apparently not correlated with the hemolytic activity and simply increased with the number of aminoethylene units without any odd−even effects.

Next, we investigated whether the protonation state of the N-substituted polyaspartamides (Figure 3) would contribute to the odd−even effect from the viewpoint of specific interactions that may lead to a disturbance in the membrane integrity. It is interesting to consider that PA-Es [PAsp(DET) and PAsp(TEP), Figure 3] at pH 5.5 contain a diprotonated state of the diaminoethane unit ($-NH_2^+-CH_2-CH_2-NH_2^+-$), corresponding to their strong hemolytic activity in acidic conditions. In contrast, no such structure is determined for PA-Os [PAsp(EDA) and PAsp(TET)] at either pH 7.4 nor 5.5 nor for PA-Es at pH 7.4, and eventually they have very limited hemolytic activity. In particular, for PAsp(TET) at pH 7.4/5.5 and PAsp(TEP) at pH 7.4, two protonated amines are spatially separated by diethyleneamine ($-CH_2-CH_2-NH-CH_2-CH_2-$) or *N,N′*-ethylene-1,2-diaminoethane ($-CH_2-CH_2-NH-CH_2-CH_2-NH-CH_2-CH_2-$) spacers. It is likely that a critical spacing length between the two protonated amino groups may exist in order to induce an effective membrane interaction. Note that an N-substituted polyaspartamide possessing a 1,3-diaminopropane unit ($-NHCH_2CH_2CH_2NH-$) in the side chain [PAsp(DPT)] assumed a fully protonated structure at pH 7.4/5.5 and induced substantial membrane destabilization of mammalian cells, as previously reported.[26] It can be assumed that two positively charged units may need to be close to each other via a spacing equivalent of approximately two or three methylene units to exert a strong interaction with cellular membranes. The additional positively charged unit in the side chain of PAsp(TEP), separated from the diprotonated diamine unit ($-NH_2^+-CH_2-CH_2-NH_2^+-$) by a flexible $-CH_2-CH_2-NH-CH_2-CH_2-$ spacer, may contribute further to enhance the binding affinity through the formation of a polyvalent charged array as multiple binding sites. This multiple binding scheme reasonably explains PAsp(TEP) polyplex's higher hemolysis efficiency as well as its enhanced endosomal escape capability compared to that of PAsp(DET) polyplex, even though the former has a lower buffering capacity than the latter.

CONCLUSION

Efficient transfection without severe cytotoxicity was achieved by the polyplexes from the N-substituted polyaspartamides possessing the even-numbered repeating aminoethylene units in their side chains [PAsp(DET) and PAsp(TEP)]. This agrees with their appreciably high buffering capacity as well as their capability to disturb the membrane integrity selectively at endosomal pH, thereby facilitating the endosomal escape of the polyplexes. Results of the hemolysis assay and the CLSM observations tracking subcellular distribution of the polyplexes suggest that two protonated amino groups may need to be tethered with critical spacing equivalent to approximately two or three methylene units to induce the strong interaction of polycations in the polyplexes with the endosomal membrane, leading to their effective transport into the cytoplasm. Importantly, fine-tuning of the number, spacing, and protonation status of repetitive amine units in the polycation side chain, as reported in this study, resolves the conflict between endosomal escape and cytotoxicity of the polyplexes, thus providing a new design concept for nonviral gene delivery systems directed toward clinical applications.

ASSOCIATED CONTENT

Supporting Information. Experimental Section and supplemental Figures 1−3. This material is available free of charge via the Internet at: http://pubs.acs.org

AUTHOR INFORMATION

Corresponding Author
kataoka@bmw.t.u-tokyo.ac.jp

ACKNOWLEDGMENT

This work was financially supported in part by the Center for Medical System Innovation (CMSI) and the Funding Program for World-Leading Innovative R&D on Science and Technology (FIRST) from Japan Society for the Promotion of Science (JSPS) and the Core Research Program for Evolutional Science and Technology (CREST) from Japan Science and Technology Agency (JST). The authors thank Kotoe Date (The University of Tokyo) for her technical assistance.

REFERENCES

(1) Mastrobattista, E.; van der Aa, M. A.; Hennink, W. E.; Crommelin, D. J. A. *Nat. Rev. Drug Discovery* **2006**, *5*, 115–121.
(2) Mintzer, M. A.; Simanek, E. E. *Chem. Rev.* **2009**, *109*, 259–302.

(3) Pack, D. W.; Hoffman, A. S.; Pun, S. *Nat. Rev. Drug Discovery* **2005**, *4*, 581–593.
(4) Wood, K. C.; Little, S. R.; Langer, R.; Hammond, P. T. *Angew. Chem., Int. Ed.* **2005**, *44*, 6704–6708.
(5) Zugates, G. T.; Anderson, D. G.; Little, S. R.; Lawhorn, I. E. B.; Langer, R. *J. Am. Chem. Soc.* **2006**, *128*, 12726–12734.
(6) Srinivasachari, S.; Fichter, K. M.; Reineke, T. M. *J. Am. Chem. Soc.* **2008**, *130*, 4618–4627.
(7) Green, J. J.; Langer, R.; Anderson, D. G. *Acc. Chem. Res.* **2008**, *41*, 749–759.
(8) Schaffert, D.; Troiber, C.; Salcher, E. E.; Frohlich, T.; Martin, I.; Badgujar, N.; Dohmen, C.; Edinger, D.; Klager, R.; Maiwald, G.; Farkasova, K.; Seeber, S.; Jahn-Hofmann, K.; Hadwiger, P.; Wagner, E. *Angew. Chem., Int. Ed.* **2011**, *50*, 1–4.
(9) Wattiaux, R.; Laurent, N.; Coninck, W. N.; Jadot, M. *Adv. Drug Delivery Rev.* **2000**, *41*, 201–208.
(10) Wagner, E.; Plank, C.; Zatloukal, K.; Cotton, M.; Birnstiel, M. L. *Proc. Natl. Acad. Sci. U. S. A.* **1992**, *89*, 7934–7938.
(11) Haensler, J.; Szoka, F. C. *Bioconjugate Chem.* **1993**, *4*, 372–379.
(12) Boussif, O.; Lezoualc'h, F.; Zanta, M. A.; Mergny, M. D.; Scherman, D.; Demeneix, B.; Behr, J. P. *Proc. Natl. Acad. Sci. U. S. A.* **1995**, *92*, 7297–7301.
(13) Midoux, P.; Monsigny, M. *Bioconjugate Chem.* **1999**, *10*, 406–411.
(14) Thomas, M.; Kilbanov, A. M. *Proc. Natl. Acad. Sci. U. S. A.* **2002**, *99*, 14640–14645.
(15) Kwon, E. J.; Bergen, J. M.; Pun, S. H. *Bioconjugate Chem.* **2008**, *19*, 920–927.
(16) Hunter, A. C. *Adv. Drug Delivery Rev.* **2006**, *58*, 1523–1531.
(17) Neu, M.; Fischer, D.; Kissel, T. *J. Gene Med.* **2005**, *7*, 992–1009.
(18) Ferrari, S.; Moro, E.; Pettenazzo, A.; Behr, J. P.; Zacchello, F.; Scarpa, M. *Gene Ther.* **1997**, *4*, 1100–1106.
(19) Wightman, L.; Kircheis, R.; Rossler, V.; Carotta, S.; Ruzicka, R.; Kursa, M.; Wagner, E. *J. Gene Med.* **2001**, *3*, 362–372.
(20) Itaka, K.; Harada, A.; Yamasaki, Y.; Nakamura, K.; Kawaguchi, H.; Kataoka, K. *J. Gene Med.* **2004**, *6*, 76–84.
(21) Densmore, C. L.; Kleinerman, E. S.; Gautam, S.; Jia, S. F.; Xu, B.; Worth, L, L.; Waldrep, J. C.; Fung, Y. K.; Ang, A, T.; Knight, V. *Cancer Gene Ther.* **2001**, *8*, 619–627.
(22) Smits, R. G.; Koper, G. J. M.; Mandel, M. *J. Phys. Chem.* **1993**, *97*, 5745–5751.
(23) Merdan, T.; Kunath, K.; Fischer, D.; Kopecek, J.; Kissel, T. *Pharm. Res.* **2002**, *19*, 140–146.
(24) Bieber, T.; Meissener, W.; Kostin, S.; Niemann, A.; Elsasser, H.-P. *J. Controlled Release* **2002**, *82*, 441–454.
(25) Walker, G. F.; Fella, C.; Pelisek, J.; Fahrmeir, J.; Boeckle, S.; Ogris, M.; Wagner, E. *Mol. Ther.* **2005**, *11*, 418–425.
(26) Miyata, K.; Oba, M.; Nakanishi, M.; Fukushima, S.; Yamasaki, Y.; Koyama, H.; Nishiyama, N.; Kataoka, K. *J. Am. Chem. Soc.* **2008**, *130*, 16287–16294.
(27) Moghimi, S. M.; Symonds, P.; Murray, J. C.; Hunter, A. C.; Debska, G.; Szewczk, A. *Mol. Ther.* **2005**, *11*, 990–995.
(28) Kanayama, N.; Fukushima, S.; Nishiyama, N.; Itaka, K.; Jang, W. D.; Miyata, K.; Yamasaki, Y.; Chung, U.; Kataoka, K. *ChemMedChem.* **2006**, *1*, 439–444.
(29) Itaka, K.; Ohaba, S.; Miyata, K.; Kawaguchi, H.; Nakamura, K.; Takato, T.; Chung, U.; Kataoka, K. *Mol. Ther.* **2007**, *15*, 1655–1662.
(30) Harada-Shiba, M.; Takamisawa, I.; Miyata, K.; Ishii, T.; Nishiyama, N.; Itaka, K.; Kangawa, K.; Yoshihara, F.; Asada, Y.; Hatakeyama, K.; Nagaya, N.; Kataoka, K. *Mol. Ther.* **2009**, *17*, 1180–1186.
(31) Arnida; Nishiyama, N.; Kanayama, N.; Jang, W.-D.; Yamasaki, Y.; Kataoka, K. *J. Controlled Release* **2006**, *115*, 208–215.
(32) Nakanishi, M.; Park, J.-S.; Jang, W.-D.; Oba, M.; Kataoka, K. *React. Funct. Polym.* **2007**, *67*, 1361–1372.
(33) Fisher, D.; Li, Y.; Ahlemeyer, B.; Kreglstein, J.; Kissel, T. *Biomaterials* **2003**, *24*, 1121–1131.